Journal of Multidisciplinary Engineering Science Studies (JMESS)
ISSN: 2458-925X
Vol. 6 Issue 9, September - 2020

CFD Studies Of Hypersonic Self-Oscillatory Flows Near Cylinders, Placed In Open Channels With Transient Cross-Sectional Area

Vladimir I. Pinchukov
Siberian branch of Russian Academy of Sc., In-te of Computational Technologies, Novosibirsk, Russia
E-mail-address: pinchvi@ict.nsc.ru

***Abstract*—Self-oscillatory hypersonic flows near cylindrical bodies, placed in open channels, are studied. Channels of rotation with the interval of cross-sectional area decreasing are considered. Two-dimensional Euler equations are solved by two methods, namely, by the explicit two step Godunov type method and by an implicit Runge-Kutta method. Smagorinsky artificial viscosity is applied in both methods to damp false fluctuations. Self-oscillatory regimes are found in CFD studies at free-stream Mach numbers of 5 to 7.5. Two types of unsteady regimes are observed.**

Keywords—Self-oscillations, Euler equations, numerical studies, channels;

I. Introduction

This paper is devoted to continuation of CFD studies of new unsteady flows, carried out in [1-6]. Namely, new family of self-oscillatory flows near pairs cylinders - open channels [6], investigated at free stream Mach numbers $3 \le M_\infty \le 4.5$, is studied here at Mach numbers $5 \le M_\infty \le 7.5$.

Self-oscillatory compressible flows may be classified into some families: 1. Flows near supersonic jets, inflowing to forward facing cavities (see, for example, [7-9]); 2. Jet impinging on a plate [1,10-14]; 3. Flows around forward-facing cavities [15-17]; 4. Tangential flows over cavities [18-21]; 5. Flows around spiked bodies [1,22-24]; 6. Flows past bluff bodies with unsteady vortex shedding [25-27]; 7. Transonic flows with bifurcations and self–oscillations near profiles [28-29].

It is generally acknowledged, that self-sustained unsteady processes arise when a positive feedback effect takes place. A search for self-oscillatory compressible flows is performed in [1-6] under supposition that resonance interactions of “active” elements of flows, namely, elements, which amplify disturbances, may be a way to realize a positive feedback effect. In any case, existence of “active” elements in a flow – contact discontinuities and intersection points of shocks with shocks or shocks with contact discontinuities – is a good criteria for a search for unsteady flows. Numerical investigations of flows, containing the most number of “active” elements [1-6], result two new families of unsteady flows. Flows near spherically blunted bodies (cylinders or cones), giving off opposite jets, are discovered to have intensive self-sustained oscillations [2-3,5]. Unsteady regimes of flows near pairs cylinders - open channels of transient cross-sectional area [6] are found for free stream Mach numbers $3 \le M_\infty \le 4.5$. These flows may contain shock waves, contact discontinuities, intersection points. CFD studies of these flows are carried out here and self-oscillations are observed for free-stream Mach numbers $5 \le M_\infty \le 7.5$.

II. CFD design approach

2.1. Boundary conditions. Fig. 1 represents schematically a numerical domain and a mesh near a cylindrical body, placed in an open channel. All variables are prescribed at the inflow boundary (*HA*). Parameters of the uniform stream are set at this boundary, namely, Mach

number $M=M_\infty$, density $\rho=1$, pressure $p=p_\infty=1$ (in dimensionless form), the radial velocity v=0. The normal velocity is equal to zero and other variables are extrapolated at solid surfaces (*CB,CD,FE,FG*). The radial velocity v=0 at the symmetry axis *HG*, other variables are extrapolated. Extrapolation conditions are used at the tube exit *DE* and at the *AB* boundary.

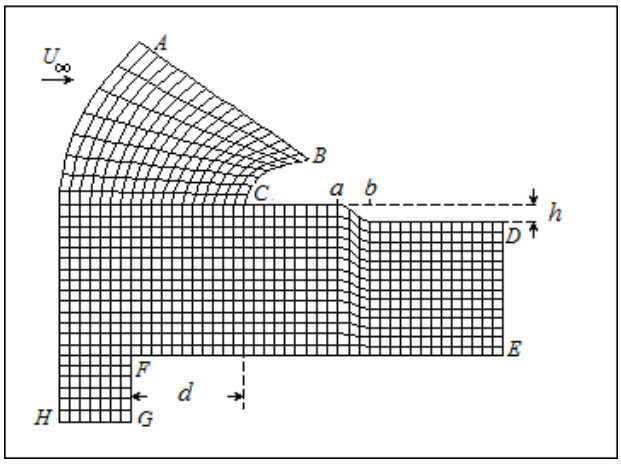

Fig. 1. Schematic representation of a numerical domain and of a mesh.

The channel form at the [*a,b*] interval of cross-sectional area decreasing is defined by the formulae

$$Y(x)=R_{tub}-16h(x-a)^2(x-2b+a)^2/(b-a)^4.$$

2.2. Numerical methods. Two methods are used.

The second order two step version of the Godunov conservative method [30] is used in majority of flow calculations. Approximate linear solution of Riemann problem is applied. Algorithms of slopes limitation of left and right extrapolation curves are used to damp false oscillations near discontinuities. Review of such algorithms of damping false oscillations is presented in [31]. Navier-Stokes viscous terms are included to Euler equations and the Smagorinsky artificial viscosity [32] is used for additional damping of false oscillations. This viscosity is calculated by equations

$$\mu=\rho|S|(C_s\Delta)^2,\ |S|=(2S_{ik}S_{ik})^{1/2},$$

$$S_{ik}=(\partial u_i/\partial x_k+\partial u_k/\partial x_i)/2,$$

$$\Delta=\Delta\xi\,\Delta\eta\,(x_\zeta y_\eta-y_\zeta x_\eta)/(\mathrm{Min}(\Delta\xi^2(x_\zeta^2+y_\zeta^2),\ \Delta\eta^2(x_\eta^2+y_\eta^2)))^{1/2},$$

where functions $x=x(\xi,\eta)$, $y=y(\xi,\eta)$ perform mapping of the unit square $\{0\le\xi\le1,\ 0\le\eta\le1\}$ to a curvilinear quadrangle on the plane of physical variables, $\Delta\xi=1/N_\zeta$, $\Delta\eta=1/N_\eta$, N_ζ, N_η - numbers of intervals of the quadrangular mesh in a unit square, C_s - constant, which is chosen in trial computations, $C_s=0.85$.

The implicit conservative Runge-Kutta method [33] is used for the accuracy control by comparing results with Godunov type method data. Written above Smagorinsky artificial viscosity terms are included in this method too. As a result the initial third order of approximation of the method [33] is reduced to the second order.

Both methods are modified here. Namely, special versions of codes are developed for the case when functions *x=x*(*a,b*), *y=y*(*a,b*) perform mapping of the unit square with excisions $\{0\le a\le a_0,\ 0\le b\le b_0\}$, $\{a_1\le a\le1,\ 0\le b\le b_1\}$ to a curvilinear quadrangle with curvilinear quadrangular excisions (see fig. 1). These versions allow carrying out calculations, described below, without dividing complicated domains into subdomains. Calculations are performed at CFL numbers from the interval [0.35,0.6], the 515×586 mesh is used usually.

Naturally, numerical calculations deal with dimensionless variables. These variables are defined as relations of initial variables and next free-stream parameters or the body size: p_∞ - for pressure, ρ_∞ - for a density, $\sqrt{p_\infty/\rho_\infty}$ - for a velocity, $r_{tub}=y(C)-y(H)$ (the maximum inner channel radius) – for space variables, $r_{tub}/\sqrt{p_\infty/\rho_\infty}$ - for time.

III. Results and discussion

Considered here flows contain at least two shock

waves. First one appears as a result of flow braking by a cylinder. Second one appears as a result of flow braking by the tube end. It is found, that self-oscillations may appear, if the relation of channel and tube lengths provides position of shock waves intersection points closed to the channel edges (signed by *C* in fig.1). The most values of self-oscillations intensities are observed in the region near this edge. So intensities at the point *C* are mainly considered below. The self-sustained fluctuations intensity is evaluated here by the density root-mean-square $\Delta\rho$:

$$\Delta\rho = \sqrt{\overline{\rho'^2}}, \qquad \overline{\rho'^2} = \sum_{n=1}^{N} (\rho_n - \overline{\rho})^2 / N, \qquad \overline{\rho} = \sum_{n=1}^{N} \rho_n / N,$$

n signs time levels.

It is found in present CFD investigations, that flow regimes depend on position intersection points of two shock waves, mentioned above, and character of this point movement. Two types of self-oscillatory flows are observed here. Next propositions on flow regimes are formulated as a result of CFD studies:

a) If intersection points of two shock waves are situated march higher or sufficiently lower of the tube edge, then flow is steady.

b) If the contact discontinuity, issued from this point, is directed always above the tube edge and moves outside a tube, a flow of the first type takes place. Nearly periodical oscillations of a moderate intensity are observed in this case. It seems, that this oscillation mechanism of the first type is similar to the oscillation mechanism in flows near spiked bodies.

c) If this contact discontinuity is directed inside or outside the tube alternately, flow contains short time peaks of pressure and density near the tube edge. These peaks appear as a result of sudden braking by the tube edge of a current, adjoined to the contact discontinuity, when this discontinuity changes direction of movement, namely, when the discontinuity starts movement upward outside of a tube. Such complicated oscillations are classified here as oscillations of the second type.

This flow physics is illustrated below by numerical examples.

Position of intersection points of two shocks waves depends significantly on geometry control parameter *d* (the cylinder and channel lengths difference). To demonstrate written above flow physics 9 flows are presented in table. These flows are defined by various values of geometrical parameters *d, a, b,* other control parameters are fixed: R_{cyl} =0.3 (cylinder radius), R_{tub} =1 (maximum inner radius of tube), $R_{\min}$ = R_{tub}-*h*=1-*h*=0.94 (the least channel radius), *h* =0.06, M_∞ =0.7 (free stream Mach number). Changeable geometrical control parameters *d*, *a*, *b* (see fig. 1) are represented in columns 2-4 of table. Results of calculations, namely, density root-mean-square magnitudes at the tube edge are shown in the fifth column of table. Godunov type method results, received for the 515×586 mesh, are used for calculations of these magnitudes.

Table. *Oscillation intensities.*

n	*d*	*a*	*B*	$\Delta\rho$
1	0.55	0.251	0.352	Steady
2	0.60	0.200	0.280	3.245
3	0.70	0.225	0.315	4.109
4	0.80	0.200	0.280	2.758
5	0.90	0.175	0.245	4.641
6	1.00	0.150	0.210	4.820
7	1.10	0.137	0.192	4.413
8	1.20	0.137	0.192	0.077
9	1.30	0.112	0.157	steady

Figs. 2 and 3 show density distributions in steady flows 1 and 9, presented in the table above. Steady regimes of these two flows are natural according to proposition a) of flow physics exposition above.

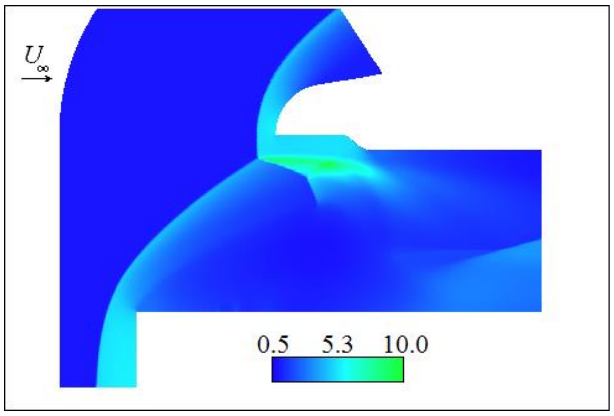

Fig. 2. The density distribution, variant 1 of table

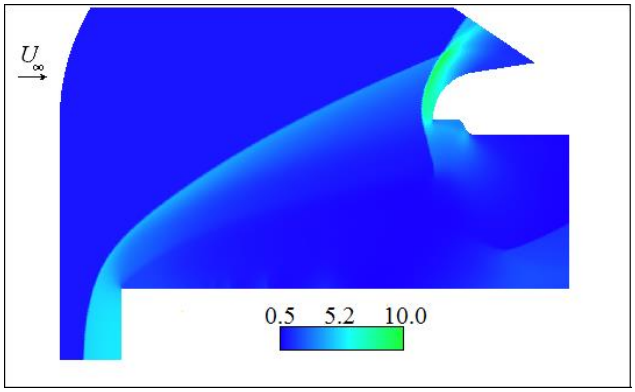

Fig. 3. The density distribution, variant 9 of table

Oscillations of two types are declared in the flow physics exposition. Figs 4-6 demonstrate first type of oscillations. Fig 4 shows density histories at the point *C* (see fig. 1) for the self-oscillatory flow number 6 in table, defined by the geometry parameter *d*=1.0 (the cylinder and channel lengths difference). Godunov type method data are marked as G. m., Runge-Kutta method data are marked as R.-K.m. The time interval, shown in fig. 4, corresponds to 48000 time steps of a numerical method.

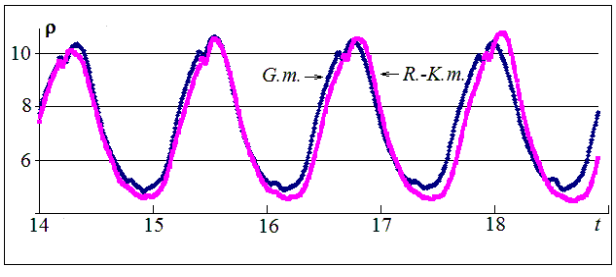

Fig. 4. Density histories, *d*=1.0.

Density histories, presented in fig. 4, illustrates that this flow is nearly periodic with the *T*=1.3 period. Godunov type method calculations are continued past the final end of fig. 4 *t*(fin) ≈18.9 through one period *T*. Density distributions for time instants *t*=18.9+*T*/4 and *t*=18.9+*T*3/4 are represented in figs. 5 and 6. These figs. correspond approximately to minimal and maximal distance of intersection point from the tube edge (point *C* in fig. 1).

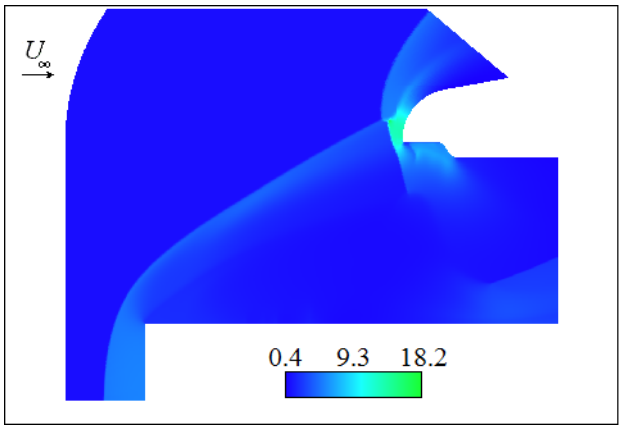

Fig. 5. The density distribution, *t*=18.9+*T*/4.

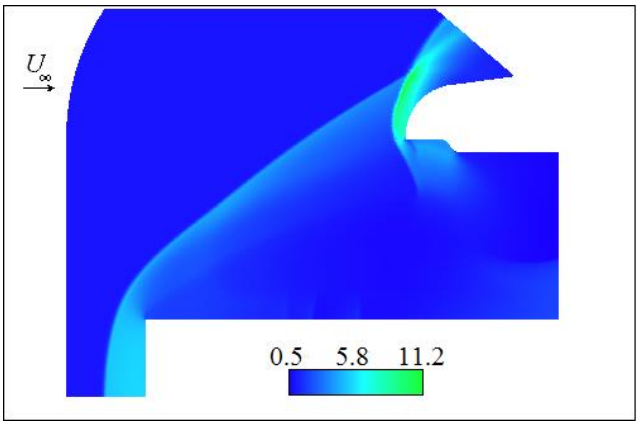

Fig. 6. The density distribution, *t*=18.9+*T*3/4.

So, if the shock waves intersection point moves always above the tube edge, flow oscillations are nearly periodic. This example illustrates point b) of flow physics propositions, presented above. It seems, that the oscillation mechanism in this case is similar to the same of flows near spiked bodies [22-24]. But the oscillation mechanism of flows near spiked bodies is not strong enough in present case and if consider the variant, which differs from the variant 6 of table (presented in figs. 4-6) only by one control parameter *h*=0 instead of *h*= 0.06, that is to say if consider straight tube, then a steady flow takes place. Some unsteady flows with different Mach numbers from the interval [5-7.5] are checked by similar way

and steady flows are resulted in every case. So, absence of the interval of cross sectional area decreasing results absence of oscillations. The question is how this area decreasing contributes to the oscillations generation? When the flow mass through a tube grows in a process of the flow dynamic, area decreasing strengthens pressure growing in a tube and, consequently, strengthens flow braking. So, area decreasing provides additional positive feed back effect, which contributes to the oscillation generation.

It is interesting to consider the neighbour variant 5 in Fig. table above. The geometry parameter d=0.9 is less then this one of the flow, considered above. So the range of shock waves intersection point movement may be waited to be nearer to the tube edge and, consequently, the type of oscillation may be changed. Fig. 7 shows the history of density magnitudes at point C for this flow. Calculations are carried out by the Godunov type method on the 515×586 mesh, 48000 time steps are performed.

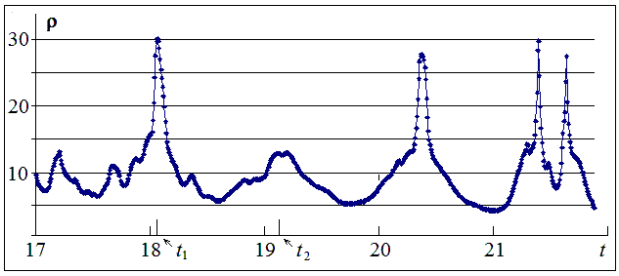

Fig. 7. The density history, d=0.9.

Peaks appearing may be seen in this fig. It seems, that peaks appear nearly periodically, but after first peak at time instant $t=t_1\approx$18.06 (see fig. 7) next peak at time instant $t=\boldsymbol{t}_2\approx$19.12 is missed by any reasons. It is interesting to see density distributions at time instants t_1 and $t=\boldsymbol{t}_2$. These distributions are shown in figs. 8 and 9. It can be seen that these figs. differ one from another mainly by position of the shock waves intersection point.

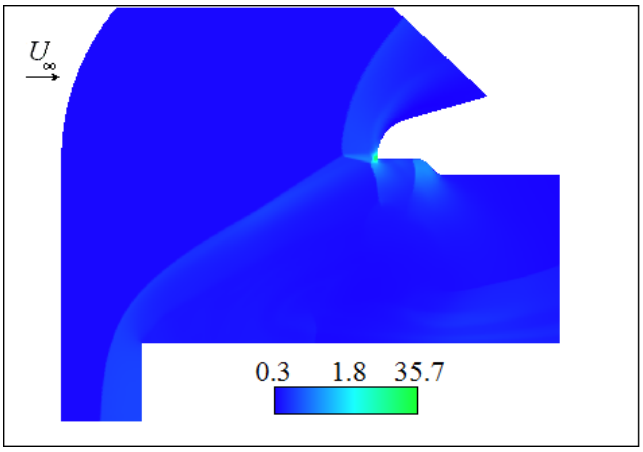

Fig. 8. Density distributions, $t=t_1$.

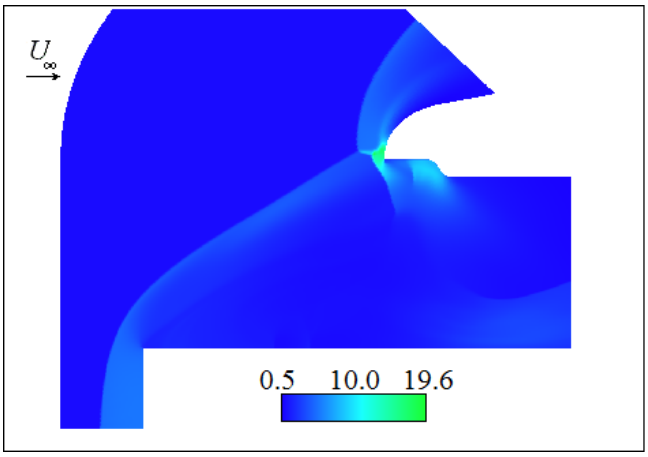

Fig. 9. Density distributions, $t=t_2$.

The question is why the density compression near the tube edge shown in fig. 8 significantly (about two times) exceeds the density compression shown in fig. 9? The shock waves intersection point, shown in fig. 9, is higher then the tube edge. It is probable that the contact discontinuity, issued from this point, was higher then the tube edge at previous time instants and, consequently, effect of current braking near the tube edge is absent. At the same time flow structure, shown in fig. 8, highly likely corresponds to the time instant after change of the contact discontinuity drift direction. If this discontinuity starts previously drifting upward, then braking had been performed and compression takes place. This explanation is based on proposition c) of flow physics exposition, presented above.

Similar flow physics are observed for other free stream Mach numbers. For example, fig. 10 shows

histories of density magnitudes at point *C* for the M_∞ =0.5 self-oscillatory flow. Calculations are carried out for geometry control parameters *d*=0.85, *a*=.197, *b*=.263, *h*=0.07, 515×586 and 715×816 meshes are used. Initial data for the second mesh are received by linear interpolation from the first mesh at time instant *t*=16. Flow modeling requires 26000 time steps for the first mesh and 34670 time steps for the second mesh. The second order Godunov type method is used.

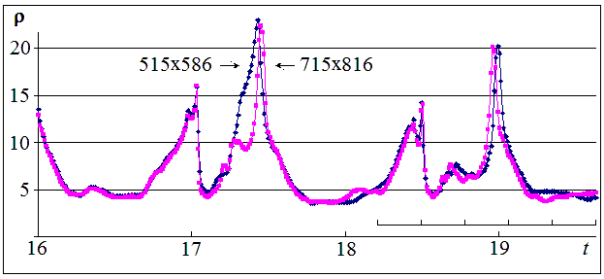

Fig. 10. Density histories for two meshes, M_∞=0.5.

Figs. 11-16 present density distributions, corresponding to time instances in the interval, shown at the bottom of fig. 10. This interval is divided into 5 subintervals. Six figs. below correspond to bounds of subintervals $t(i)=t(0)+i\tau$, $i=0,\ldots,5$, $t(0)\approx 18.21$, $\tau\approx 0.235$. The 515×586 mesh solution is shown. There is a high peak between time instants *t*(2) and *t*(3). Fig. 13, corresponding to the time instance *t*(2), shows flow structure with the shock waves intersection point, situated lower of the tube edge. Contact discontinuity, issued from this point, is situated below the tube edge. Fig. 14, corresponding to the time instance *t*(3), shows flow structure with the shock waves intersection point, situated higher of the tube edge. The contact discontinuity, issued from this point, is situated above the tube edge**.** It follows, that the contact discontinuity changes direction of propagation upward between these time instants, consequently, the current adjoined to the contact discontinuity undergoes sudden braking, which results compression, producing the density peak, visible in fig. 10 between time instants *t*(2) and *t*(3). It may be seen, that the proposition c) of the flow physics exposition, presented above, explains appearance of this peak.

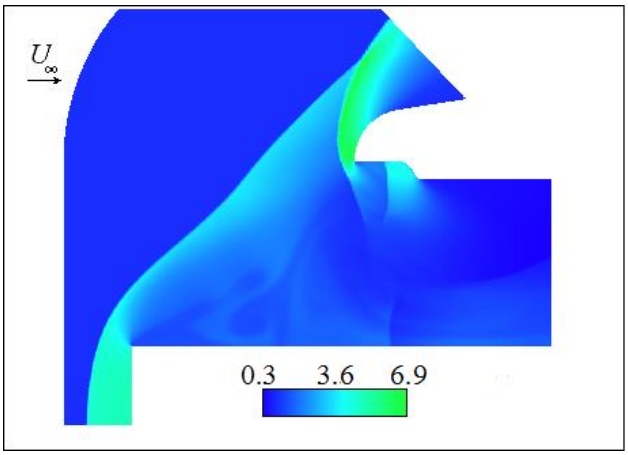

Fig. 11. The density distribution, *t*= *t*(0).

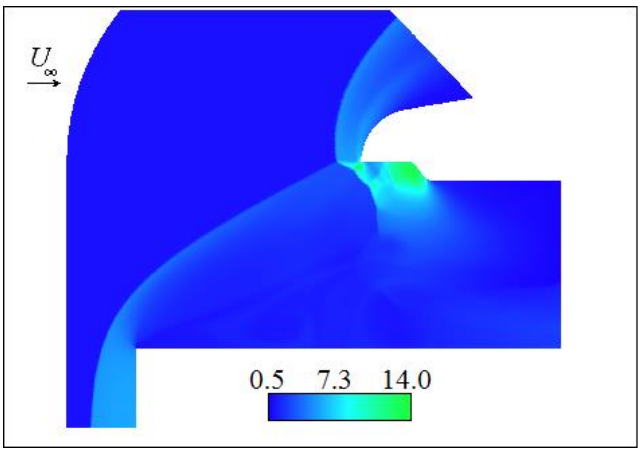

Fig. 12. The density distribution, *t*= *t*(1).

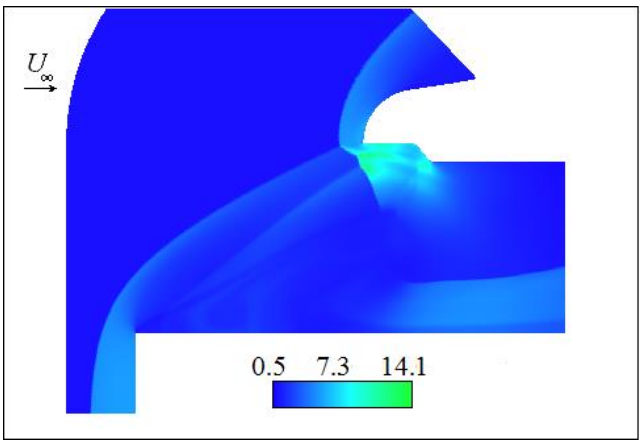

Fig. 13. The density distribution, *t*= *t*(2).

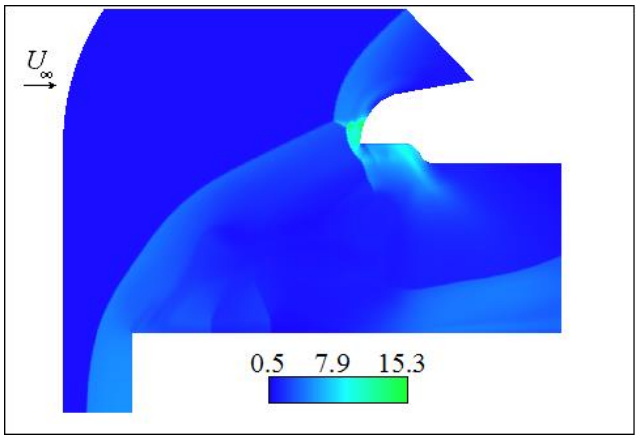

Fig. 14. The density distribution, $t = t(3)$.

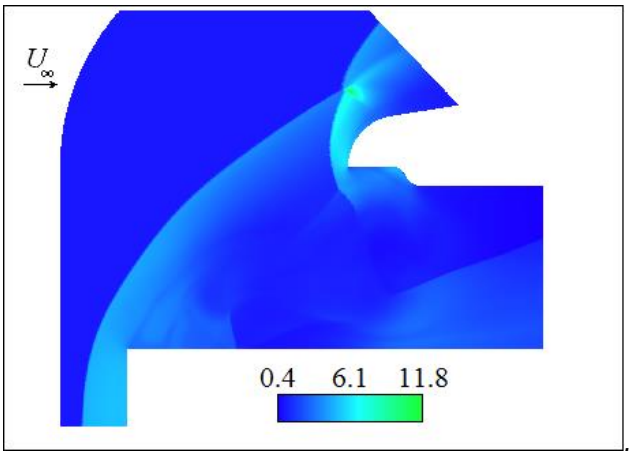

Fig. 15. The density distribution, $t=t(4)$.

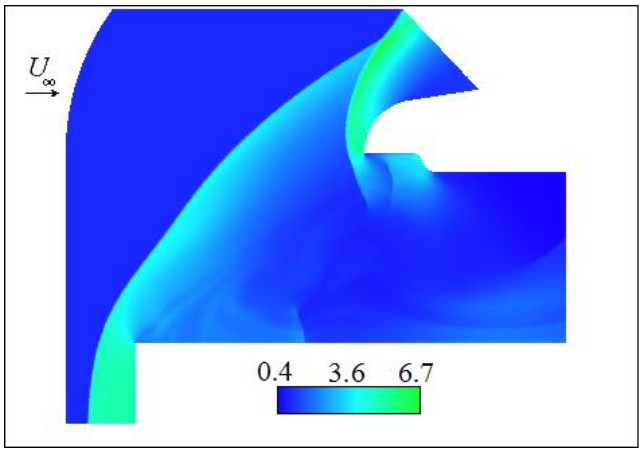

Fig. 16. The density distribution, $t=t(5)$.

IV. Conclusions

Investigations of self-oscillatory interactions of supersonic uniform streams with pairs cylindrical bodies - open channels, started in (Pinchukov, 2018), are continued here. Initial Mach numbers interval $3 \le M_\infty \le 4.5$ of unsteady regimes (Pinchukov, 2018) is extended here and self-oscillatory flows are found for Mach numbers $5 \le M_\infty \le 7.5$. Channels with the interval of cross-sectional area decreasing are considered. This decreasing is conducive to possibilities of the self-oscillatory regimes appearance.

It is found here, that unsteady regimes exist, only if intersection points of available two shock waves are not too far from the tube edge. Two types of self-oscillatory flows are observed.

If contact discontinuity, issued from the intersection point, is directed always above the tube edge, flows of the first type take place, which are nearly periodical. It seems, that the oscillation mechanism in this case is similar to the oscillation mechanism in flows near spiked bodies. The inner cylinder plays the role of a spike. But this mechanism is not strong enough and only existence of the interval of cross-sectional area decreasing, which provides additional feedback effect, may produce oscillations.

If this contact discontinuity is directed inside or outside a tube alternately, second type of unsteady flows takes place. Namely, flows contain short time peaks of pressure and density near the tube edge. These peaks appear as a result of sudden braking by the tube edge of a current, adjoined to the contact discontinuity, when this discontinuity changes direction of movement, namely, when the discontinuity starts movement upward.

References:

[1] V.I. Pinchukov, “Numerical modeling of non-stationary flows with transient regimes”, Comput. Mathem. and Mathem. Phisics, 49(10), 2009, pp. 1844–1852.

[2] V.I. Pinchukov, “Modeling of self-oscillations and a search for new self-oscillatory flows”, Mathematical Models and Computer Simulations, 4(2), 2012, pp. 170–178.

[3] V.I. Pinchukov, “Self-oscillatory flows near blunted bodies, giving off opposite jets: CFD study”, Intern. J. of Engineering and Innovative Technology, 6(5), 2016, pp. 41-46.

[4] V.I. Pinchukov, “Sonic underexpanded jet impinging on the pair open tube – inner cylinder”, Intern. J. of Modern Trends in Engineering and Research, 4(11), 2017, pp. 8-14.

[5] V.I. Pinchukov, “Godunov type methods calculations

of unsteady flows near blunted cylinders, giving off opposite jets", J. of Multidisciplinary Engineering Science Studies (JMESS), 5(10), 2019, pp. 2841-2846.

[6] V.I. Pinchukov, "Self-oscillatory interactions of supersonic streams with cylinders, placed in open channels", Intern. J. of Engineering Inventions, 7(7), 2018, pp. 16-21.

[7] J. Hartmann, "On a new method for the generation of sound waves", Phys. Rev., 20(6), 1922, pp. 719-726.

[8] S. Murugappan, E. Gutmark, "Parametric study the Hartmann–Sprenger tube", Experiments in Fluids, 38(6), 2005, pp. 813-823.

[9] J. Kastner, M. Samimy, "Development and characterization of Hartmann tube fluid actuators for high-speed control", American Institute of Aeronautics and Astronautics J., 40(10), 2012, pp. 1926–1934.

[10] W. Wu, U. Piomelli, "Large-Eddy Simulation of impinging jets with embedded azimuthal vortices", J. of Turbulence, 16(10), 2014, pp. 44-66.

[11] C.-Y. Kuo, A.P. Dowling, "Oscillations of a moderately underexpanded choked jet impinging upon a flat plate", J. Fluid Mech., 315, 1966, pp. 267–291.

[12] Y. Sakakibara, J. Iwamoto, "Numerical study of oscillation mechanism in underexpanded jet impinging on plate", J. Fluids Eng., 120, 1998, p. 477.

[13] R. Gojon, C. Bogey, "Flow structure oscillations and tone production in underexpanded impinging round jets", AIAA J., 55, 2017, pp. 1792–1805.

[14] B. Henderson, J. Bridges and M. Wernet, " An experimental study of the oscillatory flow structure of tone-producing supersonic impinging jets", J. Fluid Mech., 542, 2005, pp. 115-137.

[15] D.W. Ladoon, S.P. Schneider and J.D. Schmisseur, "Physics of resonance in a supersonic forward-facing cavity", J. of Spacecraft and Rockets, 35(5), 1998.

[16] S.I. Silton, D.B. Goldstein, "Ablation onset in unsteady hypersonic flow about nose tip with cavity", J. Thermophysics and Heat Transfer, 14(3), 2000, pp. 421-434.

[17] W.A. Engblom, B. Yuceil, D.B. Goldstein and D.S. Dolling, "Hypersonic forward-facing cavity flow: an experimental and numerical study", AIAA Paper 95-0293, 1995.

[18] J. Rossiter, "Wind-tunnel experiments on the flow over rectangular cavities at subsonic and transonic speeds", Technical Reports & Memoranda 3438. Aeronautical Research Council, 1964.

[19] C.-J. Tam, P.D. Orkwis and P.J. Disimile, "Comparison of Baldwin-Lomax turbulence models for two-dimensional open-cavity calculations", AIAA J., 34(3), Technical Notes: 629-632, 1996.

[20] H. Wang, P.Li M. Sun, and J. Wei, "Entrainment characteristics of cavity shear layers in supersonic flows", Acta Astronautica, 137, 2017, pp. 214–221.

[21] N. Murray, E. Sällström and L. Ukeiley, "Properties of subsonic open cavity flow fields", Physics of Fluids, 21, 095103-16, 2009.

[22] M. Gauer, A. Paull, "Numerical investigation of a spiked nose cone at supersonic speeds", J. of Spacecraft and Rockets, 45(3), 2008, pp. 459-471.

[23] D. Sahoo, S. Das, P. Kumar and J. Prasad, "Effect of spike on steady and unsteady flow over a blunt body at supersonic speed", Acta Astronautica, 128, 2016, pp. 521-533.

[24] R.C. Mehta, "Pressure oscillations over a spiked blunt body at hypersonic Mach number", Computational Fluid Dynamics J., 9(2), 2008, pp. 88-95.

[25] R. Natarajan, A. Acrivos, "The instability of the steady flow past spheres and disks", J. Fluid Mech., 54, 1993, pp. 333-344.

[26] E. Berger, D. Scholz and M. Schumm, "Coherent vortex structures in the wake of a sphere and a circular disk at rest and under forced vibrations", J. Fluids and Structures, 4, 1990, pp. 231-257.

[27] H. Sakamoto, H. Haniu, "The formation mechanism and shedding frequency of vortices from a sphere in uniform shear flow", J. Fluid Mech., 287, 1995, pp. 151-171.

[28] A. Jameson, "Airfoils admitting non-unique solutions of the Euler equations", Reston, Paper / AIAA; N 91-1625, 1991.

[29] M. Hafez, W.H. Guo, "Some anomalies of numerical simulation of shock waves. Pt 1. Inviscid Flows", Comput. Fluids., 28(4/5), 1999, pp. 701-719.

[30] S.K. Godunov, "A difference method for numerical calculation of discontinuous solutions of the equations of hydrodynamics", Mat. Sb. (N.S.), 47(89):3, 1959, pp. 271–306.

[31] P. Woodward, "The numerical simulation of two-dimensional fluid flow with strong shocks", Journal of Comput. Physics, 54, 1984, pp. 115-173.

[32] J. Smagorinsky, "General circulation experiments with the primitive equations. I. The basic experiment", Monthly Weather Review, 91, 1963, pp. 99-164.

[33] V.I. Pinchukov, "Numerical solution of the equations of viscous gas by an implicit third order Runge-Kutta scheme", Comput. Mathem. and Mathem. Physics, 42(6), 2002, pp. 898-907.